VOLUME 35 · NUMBER 25 · SEPTEMBER 1, 2017

JOURNAL OF CLINICAL ONCOLOGY

ORIGINAL REPORT

Therapeutic and Prognostic Implications of BRAF V600E in Pediatric Low-Grade Gliomas

Alvaro Lassaletta, Michal Zapotocky, Matthew Mistry, Vijay Ramaswamy, Marion Honnorat, Rahul Krishnatry, Ana Guerreiro Stucklin, Nataliya Zhukova, Anthony Arnoldo, Scott Ryall, Catriona Ling, Tara McKeown, Jim Loukides, Ofelia Cruz, Carmen de Torres, Cheng-Ying Ho, Roger J. Packer, Ruth Tatevossian, Ibrahim Qaddoumi, Julie H. Harreld, James D. Dalton, Jean Mulcahy-Levy, Nicholas Foreman, Matthias A. Karajannis, Shiyang Wang, Matija Snuderl, Amulya Nageswara Rao, Caterina Giannini, Mark Kieran, Keith L. Ligon, Maria Luisa Garre, Paolo Nozza, Samantha Mascelli, Alessandro Raso, Sabine Mueller, Theodore Nicolaides, Karen Silva, Romain Perbet, Alexandre Vasiljevic, Cécile Faure Conter, Didier Frappaz, Sarah Leary, Courtney Crane, Aden Chan, Ho-Keung Ng, Zhi-Feng Shi, Ying Mao, Elizabeth Finch, David Eisenstat, Bev Wilson, Anne Sophie Carret, Peter Hauser, David Sumerauer, Lenka Krskova, Valerie Larouche, Adam Fleming, Shayna Zelcer, Nada Jabado, James T. Rutka, Peter Dirks, Michael D. Taylor, Shiyi Chen, Ute Bartels, Annie Huang, David W. Ellison, Eric Bouffet, Cynthia Hawkins, and Uri Tabori

Author affiliations and support information (if applicable) appear at the end of this article.

Published at jco.org on July 20, 2017.

C.H. and U.T. contributed equally to this work.

Corresponding author: Uri Tabori, MD, Division of Haematology/Oncology, University of Toronto, Research Institute and The Arthur and Sonia Labatt Brain Tumour Research Centre, The Hospital for Sick Children, 555 University Ave, Toronto, ON, Canada, M5G 1X8; e-mail: uri.tabori@sickkids.ca.

0732-183X/17/3525w-2934w/$20.00

ABSTRACT

Purpose
BRAF V600E is a potentially highly targetable mutation detected in a subset of pediatric low-grade gliomas (PLGGs). Its biologic and clinical effect within this diverse group of tumors remains unknown.

Patients and Methods
A combined clinical and genetic institutional study of patients with PLGGs with long-term follow-up was performed (N = 510). Clinical and treatment data of patients with BRAF V600E mutated PLGG (n = 99) were compared with a large international independent cohort of patients with BRAF V600E mutated-PLGG (n = 180).

Results
BRAF V600E mutation was detected in 69 of 405 patients (17%) with PLGG across a broad spectrum of histologies and sites, including midline locations, which are not often routinely biopsied in clinical practice. Patients with BRAF V600E PLGG exhibited poor outcomes after chemotherapy and radiation therapies that resulted in a 10-year progression-free survival of 27% (95% CI, 12.1% to 41.9%) and 60.2% (95% CI, 53.3% to 67.1%) for BRAF V600E and wild-type PLGG, respectively ($P < .001$). Additional multivariable clinical and molecular stratification revealed that the extent of resection and *CDKN2A* deletion contributed independently to poor outcome in BRAF V600E PLGG. A similar independent role for *CDKN2A* and resection on outcome were observed in the independent cohort. Quantitative imaging analysis revealed progressive disease and a lack of response to conventional chemotherapy in most patients with BRAF V600E PLGG.

Conclusion
BRAF V600E PLGG constitutes a distinct entity with poor prognosis when treated with current adjuvant therapy.

J Clin Oncol 35:2934-2941. © 2017 by American Society of Clinical Oncology

INTRODUCTION

Pediatric low-grade gliomas (PLGGs) are the most frequent brain tumors in children[1] and comprise a heterogeneous group of tumors with different locations, histologic subtypes, ages at presentation,[2] and clinical behavior. In recent years, the genetic background of PLGGs[3] has begun to be unraveled. Although PLGGs are genetically quiet and each tumor harbors few genetic alterations, these ultimately converge on the activation of the RAS/MAPK pathway,[4,5] and these alterations are commonly mutually exclusive driving tumor formation. The scarcity of other genetic alterations in PLGGs is in keeping with the generally benign behavior; however, the role, if any, that these alterations play in predicting

ASSOCIATED CONTENT

Appendix
DOI: https://doi.org/10.1200/JCO.2016.71.8726

DOI: https://doi.org/10.1200/JCO.2016.71.8726

response to therapy and clinical outcome is still not known. As a result, as far as nonsurgical treatment is concerned, all patients with PLGGs receive similar treatment independent of their tumor's molecular alterations.[6] For deeply located tumors, such as hypothalamic/chiasmatic LGGs, the need for biopsy before treatment decisions are made for these children is still debated.

The BRAF V600E mutation, which is observed in a variety of adult[7] and pediatric neoplasms, is thought to be present in only a small percentage of PLGGs.[8] Controversy still exists as to whether BRAF V600E-mutant PLGG constitutes a unique subgroup with respect to natural history and outcome.[9,10] We have previously reported that PLGGs that transform to high-grade gliomas have a high incidence of BRAF V600E mutations in combination with *CDKN2A* deletion.[11] *CDKN2A* is a tumor suppressor gene and a key regulator of the cell cycle. *CDKN2A* alterations act as a secondary hit, which allows for escape from cell cycle regulation and malignant behavior in multiple cancer types.[12,13] In PLGGs, *CDKN2A* loss has been reported to be associated with escape from oncogene-induced senescence,[14] especially when combined with BRAF mutations.

To better define the clinical significance of BRAF V600E in these tumors, we performed a combined clinical and genetic analysis in an institutional discovery cohort of patients with PLGG who were diagnosed and treated in southern Ontario.[15] We then assembled a large multicenter independent cohort of patients with BRAF V600E-mutated PLGG to study their outcome and response to therapy.

PATIENTS AND METHODS

Patient Cohort

Clinical data were obtained from The Hospital for Sick Children (SickKids) institutional PLGG database, which longitudinally observes all patients in southern Ontario who were diagnosed and treated at SickKids between January 1985 and December 2015, as previously reported.[11,15]

PLGGs were defined as any glial or mixed glial-neural tumor, with the exception of ependymoma, that would be graded as grade I or II according to the revised 4th edition of the WHO Classification of Tumors of the Central Nervous System. Specifically, pleomorphic xanthoastrocytoma with anaplasia and subependymal giant-cell astrocytomas were excluded.

A discovery cohort of all patients with PLGG was assembled for which tissue and V600E mutation analysis was available (N = 510). To assess outcome and response to therapy, all 510 patients were analyzed. To adequately assess the prevalence of BRAF V600E mutations and the association with location and pathology subtypes, tumors that were diagnosed between 2000 and 2015 (n = 449) were analyzed, as 90% of the patients (n = 405) had available molecular data to test for PLGG mutations (Table 1). For outcome of BRAF V600E PLGG, an independent cohort of patients with BRAF V600E-mutated PLGG was assembled from 18 collaborating international pediatric centers. The study was approved by the SickKids research ethics board and that of all participating institutions.

The extent of surgical resection, radiation, and chemotherapy data and their association with outcome were assessed in both the SickKids cohort and independent cohort. To assess the response to chemotherapy, imaging findings before and 6 months after the initiation of treatment were compared. Progression was defined as the need for treatment change (ie, surgery, alternate chemotherapy, or radiation) related to tumor progression on imaging and/or clinical worsening, as previously described.[16-18]

Table 1. Patient and Tumor Characteristics in the SickKids Cohort (patients from 2000 to 2015)

Characteristic	All Patients (N = 405)	WT (n = 336; 83%)	V600E Mutant (n = 69; 17%)
Sex, %			
Male/female	50.6/49.4	51.2/48.8	47.8/52.2
Age, years			
Median	8.52	8.08	11.1
Range	0-18.28	0.52-18.28	0-17.46
25th/75th quartile	4.34/12.55	4.05/12.02	6.5/14.32
Location, No. (%)			
Hemispheric	157 (100)	114 (72.6)	43 (27.4)
Diencephalic	74 (100)	61 (82.4)	13 (17.6)
Brainstem	39 (100)	33 (84.6)	6 (15.4)
Cerebellum	112 (100)	108 (96.4)	4 (3.6)
Spine	15 (100)	12 (80)	3 (20)
Disseminated	8 (100)	8 (100)	0 (0)
Pathology, No. (%)			
Pilocytic astrocytoma	167 (100)	162 (97)	5 (3)
Pilomyxoid astrocytoma	15 (100)	13 (86.7)	2 (13.3)
Ganglioglioma	51 (100)	26 (51)	25 (49)
PXA	9 (100)	2 (22.2)	7 (77.8)
Diffuse astrocytoma	23 (100)	13 (56.5)	10 (43.5)
LGG NOS	70 (100)	56 (80)	14 (20)
Others	70 (100)	64 (91.4)	6 (8.6)

Abbreviations: LGG NOS, low-grade glioma not otherwise specified; PXA, pleomorphic xanthoastrocytoma, WT, wild type.

Molecular Analysis

For the SickKids cohort, BRAF V600E mutations were determined by Droplet Digital (DD)-PCR (Bio-Rad, Hercules, CA) and/or by a Clinical Laboratory Improvement Amendments–approved immunohistochemistry test. For the independent cohort, V600E mutations were analyzed using institutional Clinical Laboratory Improvement Amendments–approved tests. KIAA1549-BRAF fusion and/or BRAF duplication were evaluated using NanoString (NanoString, Seattle, WA) and/or fluorescent in situ hybridization as described previously.[16,19]

CDKN2A was analyzed using DD-PCR, single-nucleotide polymorphism array, or FISH for all available samples. For the independent cohort, if *CDKN2A* was not analyzed locally, we performed the assay using DD-PCR. We defined *CDKN2A* deletion as two copy loss by fluorescent in situ hybridization or the relative value that correlates with two copy loss as analyzed by single-nucleotide polymorphism array or DD-PCR, taking into account normal cell infiltration. Additional information on clinical and molecular parameters is available in the Appendix (online only).

Statistical Analysis

Progression-free survival (PFS) was defined as the interval between initial diagnosis and the time of progression. Overall survival (OS) was calculated as the time from diagnosis to the time of death from any cause as reported by the referring institution.

PFS and OS were analyzed by the Kaplan-Meier method, and *P* values are reported using the log-rank test. Survival data are presented as survival estimates, including 95% CIs. Associations between covariates and risk groups were tested by using Fisher's exact test. Univariable and multivariable Cox proportional hazards regression was used to estimate hazard ratios (HRs), including 95% CIs. All *P* values reported are two sided. All statistical analyses were performed with the R statistical environment (version 3.1.2), using R packages survival (version 2.37-7), Regression Modeling Strategies (version 4.3-1), Cox Regression with Firth's Penalized Likelihood (version 1.1), and Create Elegant Data Visualisations Using Grammar of Graphics (version 1.0.0), as well as SAS (SAS/STAT User's Guide, version 9.4; SAS Institute, Cary, NC).

RESULTS

BRAF V600E Is Common in PLGG

Among the 405 patients with PLGG who were treated at SickKids between 2000 and 2015, 69 (17%) harbored the BRAF V600E mutation. This analysis included all tumors and not only patients who required additional postoperative treatment. BRAF V600E tumors were diagnosed in all ages and originated from all CNS locations (Table 1). Of importance, the mutation was common in midline tumors, including optic pathway, brainstem, and spinal cord tumors. Overall, 33% of BRAF V600E PLGGs originated in the midline (diencephalon and brainstem). Similarly, BRAF V600E mutations were observed in most pathologic subtypes. As expected, the highest incidence of the mutation was observed in pleomorphic xanthoastrocytoma (78%) followed by gangliogliomas (49%); however, the mutation was also commonly observed in diffuse astrocytomas (43%) and WHO grade I astrocytomas (20%; Table 1).

BRAF V600E Mutation Confers Poor Outcome With Conventional Therapies

Long-term survival data were analyzed in 510 patients with PLGG from the SickKids cohort (mean follow-up, 7 years; range, 0.01 to 28 years).[15] In contrast to other PLGGs, BRAF V600E-mutant tumors (n = 99) continued to progress without reaching a plateau. Five-year PFS for BRAF V600E-mutant and wild-type (WT) PLGG was 50.1% (95% CI, 38.1% to 62.1%) and 72.8% (95% CI, 67.9% to 77.7%), respectively. Furthermore, 10-year PFS for BRAF V600E-mutant and WT PLGG was 27% (95% CI, 12.1% to 41.9%) and 60.2% (95% CI, 53.3% to 67.1%), respectively (HR, 2.04; 95% CI, 1.45 to 2.88; $P < .001$; Fig 1A). Continuous late progression was associated with late deaths in patients with the BRAF-V600E PLGG. Ten-year OS for BRAF V600E and WT PLGG was 83.9% (95% CI, 72.5% to 95.6%) and 92.1% (95% CI, 88.6% to 95.6%), respectively (HR, 1.57; 95% CI, 0.80 to 3.14; $P = .183$; Fig 1B). Of importance, late deaths related to tumor progression were observed in BRAF V600E PLGG even at 25 years of follow-up. Furthermore, survival

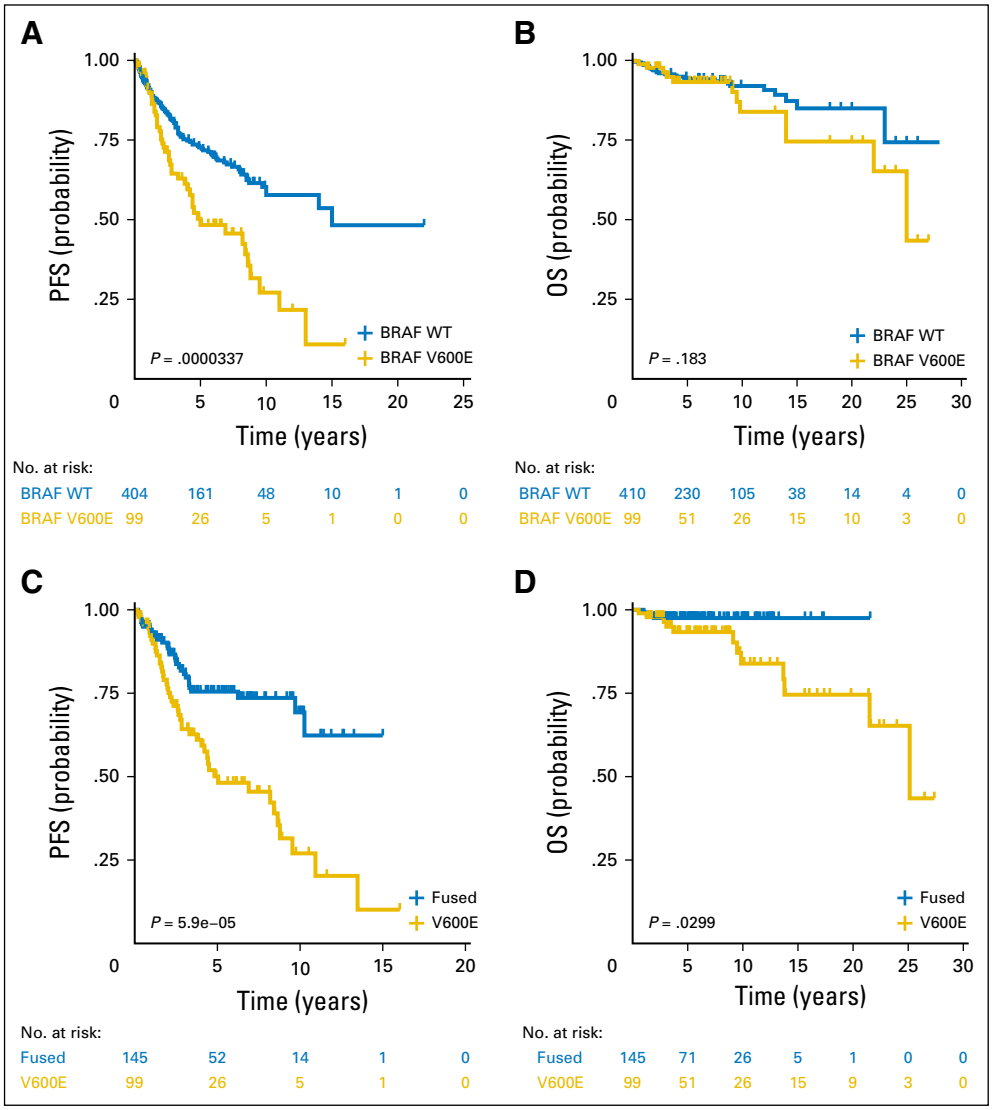

Fig 1. Survival of patients from the SickKids cohort with pediatric low-grade glioma stratified by BRAF V600E status. (A) Progression-free survival (PFS) of the SickKids cohort according to BRAF V600E status. (B) Overall survival (OS) for the entire SickKids cohort according to BRAF V600E status. (C) PFS of the SickKids cohort comparing BRAF V600E with KIAA1549-BRAF. (D) OS of the SickKids cohort comparing BRAF V600E with KIAA1549-BRAF. *P* values were determined by using the log-rank test. WT, wild type.

analysis revealed that patients with BRAF V600E PLGG faired significantly worse than those with the BRAF KIAA1549 fusion (Figs 1C and 1D).

To further examine the causes of poor survival in children with BRAF V600E-mutant PLGG, the effect of current therapeutic interventions in the SickKids cohort were tested. Despite gross total resection (GTR), which was achieved in 44.4% of these tumors, many patients with BRAF V600E PLGG continued to experience progression postresection. Five-year PFS for GTR and non-GTR was 67.8% (95% CI, 46.8% to 88.8%) and 38.8% (95% CI, 24.1% to 53.5%), respectively ($P = .01$; Fig 2A). These findings are in keeping with analysis performed in BRAF WT PLGG in which we observed a 5-year PFS of 95.9% (95% CI, 92.5% to 99.6%) for GTR and 53.3% (95% CI, 46% to 61.7%) for non-GTR ($P < .001$). Strikingly, PFS was much worse in patients with BRAF V600E PLGG who achieved GTR compared with patients with BRAF WT PLGG ($P < .001$). Similarly, patients with BRAF V600E PLGG experienced poor outcome postradiation and chemotherapy. Five- and 10-year PFS postradiotherapy was 42.2% (95% CI, 20.6% to 63.8%) and 28.1% (95% CI, 6.7% to 49.5%), respectively (Appendix Fig A1A, online only). Thirty-two percent of patients with BRAF V600E-mutant received chemotherapy. Five-year PFS after first-line chemotherapy was 30.4% (95% CI, 13.3% to 47.5%; Appendix Fig A1B).

Copy number status of *CDKN2A* was available for 403 patients with PLGG from the SickKids cohort. *CDKN2A* was deleted in 25% of BRAF V600E PLGGs and 17% of WT PLGGs. Although *CDKN2A* deletion resulted in poor survival and PFS for the entire cohort, this effect was restricted to BRAF V600E PLGGs (Appendix Fig A2, online only). PFS in children with BRAF V600E PLGG was 24.0% (95% CI, 1.9% to 46.1%) and 68.7% (95% CI, 52.8% to 70.2%) for the *CDKN2A* deleted and balanced tumors, respectively, at 5 years and 0% and 45.9% (95% CI, 21.6% to 70.2%), respectively, at 10 years ($P = .005$; Fig 2C).

To further examine the poor outcome observed in patients with BRAF V600E PLGG in the SickKids cohort, an independent cohort of 180 patients with BRAF V600E PLGG was compiled from 18 large, pediatric neuro-oncology centers. Characteristics of the independent cohort compared with SickKids patient cohort with

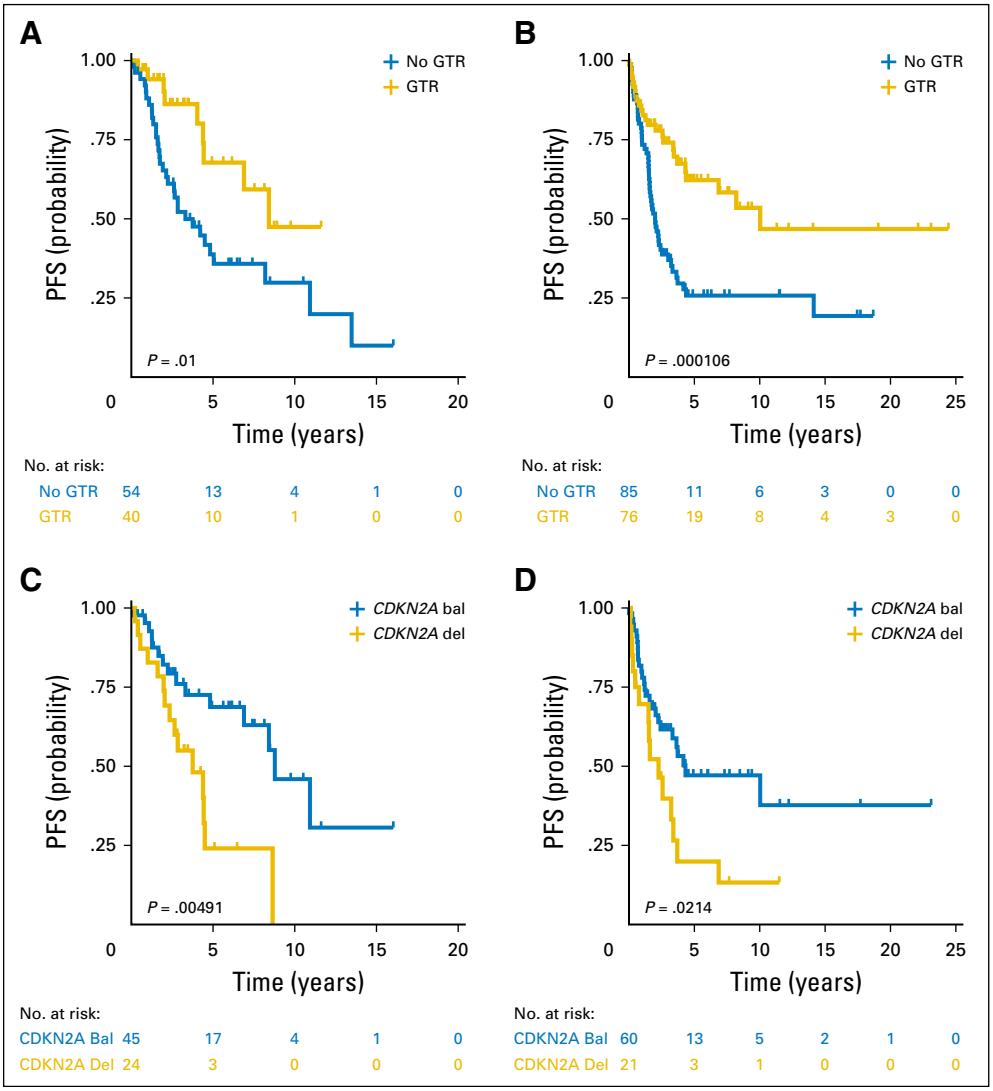

Fig 2. Survival of patients with BRAF V600E pediatric low-grade glioma according to the extent of resection and *CDKN2A* deletion. (A) Progression-free survival (PFS) of the BRAF V600E SickKids cohort according to the extent of resection. (B) PFS for the BRAF V600E independent cohort according to the extent of resection. (C) PFS for the BRAFV 600E SickKids cohort according to *CDKN2A* status. (D) PFS for the BRAF V600E independent cohort according to *CDKN2A* status. *P* values were determined using the log-rank test. GTR, gross total resection. bal, balanced; del, deleted.

Table 2. Multivariable Analysis

Variable	HR	95% CI	*P*
SickKids discovery cohort			
PFS			
BRAF V600E	1.5964	1.0054 to 2.535	.0474
CDKN2A deleted	1.4882	0.9203 to 2.406	.1050
Age	0.9682	0.9251 to 1.013	.1657
Subtotal resection	6.3849	3.7810 to 10.782	4.05×10^{-12}
Female sex	1.2525	0.8472 to 1.852	.259
Grade 2	1.2084	0.6020 to 2.426	.5944
OS			
BRAF V600E	1.1278	0.62 to 2.051	.6936
CDKN2A deleted	0.9681	0.4946 to 1.895	.9246
Age	0.9604	0.9161 to 1.007	.0940
Subtotal resection	6.4670	3.8284 to 10.924	2.98×10^{-12}
Female sex	1.2235	0.8283 to 1.807	.3108
Grade 2	1.0232	0.5005 to 2.092	.9499
BRAF V600E: *CDKN2A*	3.2550	1.1332 to 9.35	.0284
Independent cohort			
PFS			
CDKN2A deleted	2.283	1.25 to 4.170	.00722
Subtotal resection	1.950	1.091 to 3.484	.02414
OS			
CDKN2A deleted	4.342	1.0659 to 17.688	.0405
Subtotal resection	1.954	0.4611 to 8.279	.3633

Abbreviations: HR, hazard ratio; OS, overall survival; PFS, progression-free survival.

the V600E mutation are listed in Appendix Table A1. Overall, similar poor PFS and OS were observed in patients with the BRAF V600E mutation (Appendix Fig A3, online only). Of importance, as observed in the discovery cohort, a lack of complete resection was associated with poor outcome in patients with BRAF V600E PLGG ($P = .001$; Fig 2B), and *CDKN2A* deletion also conferred poor outcome in the independent cohort ($P = 0.02$; Fig 2D).

An Integrative Prognostic Model for BRAF V600E PLGG

Combining the extent of resection, BRAF V600E and *CDKN2A* deletion revealed a high-risk group of patients with PLGG. In a multivariable Cox proportional hazards regression model of the discovery cohort, BRAF V600E and the extent of resection contributed independently to outcome. Moreover, when interaction between BRAF V600E and *CDKN2A* status was implemented, the combination of BRAF V600E and *CDKN2A* deletion predicted recurrence with an HR of 3.2 ($P = .03$; Table 2). Similarly, the extent of resection and *CDKN2A* status were independent predictors of poor outcome in the BRAF V600E independent cohort. Five-year PFS for patients with BRAF V600E and *CDKN2A* deletion and non-GTR in the SickKids cohort and independent cohort was 24% (95% CI, 1.9% to 46.1%) and 15% (95% CI, 0% to 42%) respectively. Using c-statistics analysis, the addition of BRAF V600E slightly improved the prediction model expressed by nonsignificant change in area under the curve from 0.814 to 0.826 ($P = .668$).

BRAF V600E PLGG Responds Favorably to Targeted Therapy

Six patients with BRAF V600E-mutated PLGG who experienced progression after conventional treatment were treated with BRAF inhibitors on a compassionate basis. Because targeted therapies represent a novel and attractive option for progressive BRAF V600E cancers,[20] quantitative imaging findings at 6 months from initiation of conventional chemotherapy and targeted therapy were compared for the SickKids cohort and independent cohort. At 6 months, only 23% of tumors revealed an objective response to chemotherapy (> 25% of tumor shrinkage). Furthermore, up to 24% of the tumors progressed while on therapy, which resulted in treatment changes. This did not differ between first-line, second-line, and third-line chemotherapy. Of interest, all six progressive tumors, which were treated with V600E inhibitors, showed significant response (49% to 80% cytoreduction) to targeted therapy (Fig 3). All six patients remain on V600E inhibitors to date with a median follow-up of 18.5 months (range, 15 to 36 months). In one patient, the V600E inhibitor was discontinued after 2 years. This patient developed a significant tumor progression associated with clinical deterioration. Therapy was restarted with rapid clinical and radiologic responses.

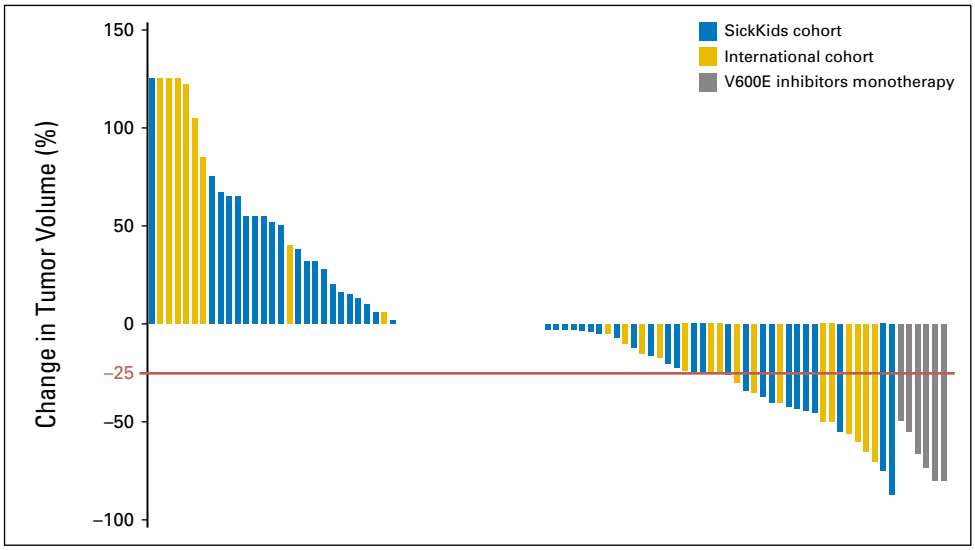

Fig 3. Response of patients with BRAF V600E pediatric low-grade glioma to chemotherapy and BRAF V600E inhibition. Waterfall plot of response to chemotherapy at 6 months. Note the response to BRAF V600E inhibitors in gray. PFS, progression-free survival.

DISCUSSION

This study explores a specific type of molecularly defined subgroup of PLGG. BRAF V600E is more common than originally thought in PLGG[21]—17% of cases—and is relatively common in previously unrecognized locations, such as the midline. BRAF V600E confers worse outcomes when treated with chemotherapy and radiation compared with BRAF WT PLGG, especially when *CDKN2A* deletion coexists. It also highlights several important observations that may affect our approach to and management of these tumors.

Although BRAF V600E is known to be common in pleomorphic xanthoastrocytoma and gangliogliomas,[21-23] this mutation is not restricted to those histologic subtypes and is highly prevalent in diffuse astrocytomas and other low-grade astrocytomas (Table 1). This is in agreement with other smaller series that have reported V600E in all PLGG subtypes.[24,25] Of importance, BRAF V600E mutation can be found in any location in the CNS, and > 33% of BRAF V600E-mutant tumors are located in the midline (diencephalon and brainstem). Tumors in these locations are often not biopsied, and medical therapy (radiation and chemotherapy) is initiated blindly under the assumption that all PLGGs will have similar outcome.[26-28] Furthermore, because in some cases a gray zone exists between low-grade and high-grade glioma in children, and a histopathologic definition is not universally suitable to distinguish these, molecular analysis adds an important dimension to the approach for such tumors. Together, as BRAF V600E represents a clinically distinct subgroup of PLGG, current approaches toward the need for biopsy and molecular testing in PLGG should be re-evaluated.

Overall, our data suggest that BRAF V600E and *CDKN2A* deletion constitute a distinct clinical entity within PLGG. First, as observed in both the SickKids cohort and independent cohort (Fig 2), these tumors are relentless and tend to recur multiple times, which results in poor outcome, which is dissimilar to other PLGGs. Extensive clinical follow-up enabled through the Ontario databases allows for the capture of late deaths observed in patients with BRAF V600E PLGG. These represent a major burden that extends from childhood to adult survivors of PLGG.[15] These late deaths are attributed to late progression and tumor transformation up to 25 years after initial diagnosis.[11] Second, BRAF V600E PLGGs represent a distinct entity in their poor outcome after current conventional therapies. After complete resection, typical PLGGs do not need additional treatment—only 5% of WT tumors with GTR in the SickKids cohort recurred. One third of BRAF V600E PLGG in which GTR was achieved recurred in both the SickKids cohort and independent cohort (Figs 2A and 2B), which suggests different tumor invasiveness.

For PLGG as a whole, outcome after radiation and chemotherapy is associated with PFS > 80% and 50%, respectively, at 5 years in PLGG series.[27,29,30] In contrast, the present experience shows that BRAF V600E PLGGs have < 50% and 35% PFS after radiation and chemotherapy, respectively, at 5 years (Appendix Fig A1). Together, this suggests a different tumor type.

CDKN2A alterations are common in many adult cancers, including gliomas.[12,13] It allows for a bypass of cell cycle arrest, which would normally be initiated by RAS pathway oncogenic activation.[14] In contrast to adult gliomas, *TP53* mutations are uncommon in PLGGs; therefore, *CDKN2A* alterations may play an important role in the behavior of some of these tumors. In this study, *CDKN2A* deletion conferred poor outcome for patients with PLGG who harbored the BRAF V600E mutation. The prognostic value of this alteration was confirmed in the independent cohort.

Combining V600E, *CDKN2A*, and the extent of resection, we are able to define a high-risk group of PLGG with < 10% chance of tumor control and poor survival with conventional therapies. These survival curves are not observed in other PLGGs, and novel therapies should be considered for these patients.

Analysis of tumor response within 6 months of initiation in those who received chemotherapy provided important insight into the clinical behavior of BRAF V600E PLGG. A significant proportion of these patients had to switch to other chemotherapy regimens or radiation at 6 months as a result of tumor progression. This is rarely observed with current PLGG protocols.[17,27] Although the numbers are small and should still be considered anecdotal, all six patients who were treated with a BRAF V600E inhibitor achieved a response, with volumetric shrinkage of 49% to 80% with this targeted therapy. This objective response is encouraging in view of previous data. Of note, remarkable clinical improvement was observed in all these heavily pretreated patients.[31]

Results of clinical trials that used BRAF V600E inhibitors in patients with PLGG are pending; however, several case reports have already shown activity of BRAF V600E inhibitors in children with PLGG.[31-35] Although longer follow-up is required to determine emerging resistance and long-term adverse effects of these drugs, the rapid responses observed with these therapies in patients with BRAF V600E PLGG are encouraging and can potentially prevent ongoing sequelae, such as visual loss and neurologic deterioration, which are commonly observed with current therapies.

Taken together, these data reveal that BRAF V600E PLGGs are distinct from other PLGGs and require a different short-term and long-term therapeutic approach. Upfront diagnosis of these tumors is needed to define prognosis and a decision whether to include aggressive surgery and early targeted therapies for these patients. Finally, this study highlights the need for a change in our overall approach to PLGGs. Consideration for upfront biopsy and molecular diagnosis of deeply located midline tumors that are commonly treated without histologic confirmation will allow for better tailoring of therapeutic interventions and better outcome for these children in the era of precision medicine.

AUTHORS' DISCLOSURES OF POTENTIAL CONFLICTS OF INTEREST

Disclosures provided by the authors are available with this article at jco.org.

AUTHOR CONTRIBUTIONS

Conception and design: Alvaro Lassaletta, Michal Zapotocky, Matthew Mistry, Rahul Krishnatry, Ana Guerreiro Stucklin, Eric Bouffet, Cynthia Hawkins, Uri Tabori

Provision of study materials or patients: Romain Perbet, Adam Fleming

Collection and assembly of data: Alvaro Lassaletta, Michal Zapotocky, Matthew Mistry, Vijay Ramaswamy, Marion Honnorat, Rahul Krishnatry, Ana Guerreiro Stucklin, Nataliya Zhukova, Anthony Arnoldo, Scott Ryall, Catriona Ling, Tara McKeown, Jim Loukides, Ofelia Cruz, Carmen de Torres, Cheng-Ying Ho, Roger J. Packer, Ruth Tatevossian, Ibrahim Qaddoumi, Julie H. Harreld, James D. Dalton, Jean Mulcahy-Levy, Nicholas Foreman, Matthias A. Karajannis, Shiyang Wang, Matija Snuderl, Amulya Nageswara Rao, Caterina Giannini, Mark Kieran, Keith L. Ligon, Maria Luisa Garre, Paolo Nozza, Samantha Mascelli, Alessandro Raso, Sabine Mueller, Theodore Nicolaides, Karen Silva, Romain Perbet, Alexandre Vasiljevic, Cécile Faure Conter, Didier Frappaz, Sarah Leary, Courtney Crane, Aden Chan, Ho-Keung Ng, Zhi-Feng Shi, Ying Mao, Elizabeth Finch, David Eisenstat, Bev Wilson, Anne Sophie Carret, Peter Hauser, David Sumerauer, Lenka Krskova, Valerie Larouche, Adam Fleming, Shayna Zelcer, Nada Jabado, James T. Rutka, Peter Dirks, Michael D. Taylor, Ute Bartels, Annie Huang, David W. Ellison, Eric Bouffet, Cynthia Hawkins, Uri Tabori
Data analysis and interpretation: Alvaro Lassaletta, Michal Zapotocky, Matthew Mistry, Vijay Ramaswamy, Ana Guerreiro Stucklin, Catriona Ling, Shiyi Chen, Eric Bouffet, Cynthia Hawkins, Uri Tabori
Manuscript writing: All authors
Final approval of manuscript: All authors
Accountable for all aspects of the work: All authors

REFERENCES

1. Ostrom QT, Gittleman H, Fulop J, et al: CBTRUS statistical report: Primary brain and central nervous system tumors diagnosed in the United States in 2008-2012. Neuro-oncol 17:iv1-iv62, 2015 (Suppl 4)
2. Sievert AJ, Fisher MJ: Pediatric low-grade gliomas. J Child Neurol 24:1397-1408, 2009
3. Bergthold G, Bandopadhayay P, Bi WL, et al: Pediatric low-grade gliomas: How modern biology reshapes the clinical field. Biochim Biophys Acta 1845:294-307, 2014
4. Jones DT, Hutter B, Jäger N, et al: Recurrent somatic alterations of FGFR1 and NTRK2 in pilocytic astrocytoma. Nat Genet 45:927-932, 2013
5. Zhang J, Wu G, Miller CP, et al: Whole-genome sequencing identifies genetic alterations in pediatric low-grade gliomas. Nat Genet 45: 602-612, 2013
6. Bergthold G, Bandopadhayay P, Hoshida Y, et al: Expression profiles of 151 pediatric low-grade gliomas reveal molecular differences associated with location and histological subtype. Neuro-oncol 17: 1486-1496, 2015
7. Romano E, Schwartz GK, Chapman PB, et al: Treatment implications of the emerging molecular classification system for melanoma. Lancet Oncol 12:913-922, 2011
8. Horbinski C, Nikiforova MN, Hagenkord JM, et al: Interplay among BRAF, p16, p53, and MIB1 in pediatric low-grade gliomas. Neuro-oncol 14:777-789, 2012
9. Dahiya S, Haydon DH, Alvarado D, et al: BRAF (V600E) mutation is a negative prognosticator in pediatric ganglioglioma. Acta Neuropathol 125:901-910, 2013
10. Ho CY, Mobley BC, Gordish-Dressman H, et al: A clinicopathologic study of diencephalic pediatric low-grade gliomas with BRAF V600 mutation. Acta Neuropathol 130:575-585, 2015
11. Mistry M, Zhukova N, Merico D, et al: BRAF mutation and CDKN2A deletion define a clinically distinct subgroup of childhood secondary high-grade glioma. J Clin Oncol 33:1015-1022, 2015
12. Berg M, Nordgaard O, Kørner H, et al: Molecular subtypes in stage II-III colon cancer defined by genomic instability: Early recurrence-risk associated with a high copy-number variation and loss of RUNX3 and CDKN2A. PLoS One 10:e0122391, 2015
13. Alhejaily A, Day AG, Feilotter HE, et al: Inactivation of the CDKN2A tumor-suppressor gene by deletion or methylation is common at diagnosis in follicular lymphoma and associated with poor clinical outcome. Clin Cancer Res 20:1676-1686, 2014
14. Jacob K, Quang-Khuong DA, Jones DT, et al: Genetic aberrations leading to MAPK pathway activation mediate oncogene-induced senescence in sporadic pilocytic astrocytomas. Clin Cancer Res 17: 4650-4660, 2011
15. Krishnatry R, Zhukova N, Guerreiro Stucklin AS, et al: Clinical and treatment factors determining long-term outcomes for adult survivors of childhood low-grade glioma: A population-based study. Cancer 122:1261-1269, 2016
16. Hawkins C, Walker E, Mohamed N, et al: BRAF-KIAA1549 fusion predicts better clinical outcome in pediatric low-grade astrocytoma. Clin Cancer Res 17:4790-4798, 2011
17. Lassaletta A, Scheinemann K, Zelcer SM, et al: Phase II weekly vinblastine for chemotherapy-naïve children with progressive low-grade glioma: A Canadian Pediatric Brain Tumor Consortium study. J Clin Oncol 34:3537-3543, 2016
18. Bouffet E, Jakacki R, Goldman S, et al: Phase II study of weekly vinblastine in recurrent or refractory pediatric low-grade glioma. J Clin Oncol 30:1358-1363, 2012
19. Ryall S, Krishnatry R, Arnoldo A, et al: Targeted detection of genetic alterations reveal the prognostic impact of H3K27M and MAPK pathway aberrations in paediatric thalamic glioma. Acta Neuropathol Commun 4:93, 2016
20. Abraham J, Stenger M: Dabrafenib in advanced melanoma with BRAF V600E mutation. J Community Support Oncol 12:48-49, 2014
21. Schindler G, Capper D, Meyer J, et al: Analysis of BRAF V600E mutation in 1,320 nervous system tumors reveals high mutation frequencies in pleomorphic xanthoastrocytoma, ganglioglioma and extracerebellar pilocytic astrocytoma. Acta Neuropathol 121:397-405, 2011
22. Dougherty MJ, Santi M, Brose MS, et al: Activating mutations in BRAF characterize a spectrum of pediatric low-grade gliomas. Neuro-oncol 12: 621-630, 2010
23. Dias-Santagata D, Lam Q, Vernovsky K, et al: BRAF V600E mutations are common in pleomorphic xanthoastrocytoma: Diagnostic and therapeutic implications. PLoS One 6:e17948, 2011
24. Qaddoumi I, Orisme W, Wen J, et al: Genetic alterations in uncommon low-grade neuroepithelial tumors: BRAF, FGFR1, and MYB mutations occur at high frequency and align with morphology. Acta Neuropathol 131:833-845, 2016
25. Dimitriadis E, Alexiou GA, Tsotsou P, et al: BRAF alterations in pediatric low-grade gliomas and mixed neuronal-glial tumors. J Neurooncol 113:353-358, 2013
26. Gururangan S, Fisher MJ, Allen JC, et al: Temozolomide in children with progressive low-grade glioma. Neuro-oncol 9:161-168, 2007
27. Ater JL, Zhou T, Holmes E, et al: Randomized study of two chemotherapy regimens for treatment of low-grade glioma in young children: A report from the Children's Oncology Group. J Clin Oncol 30: 2641-2647, 2012
28. Packer RJ, Lange B, Ater J, et al: Carboplatin and vincristine for recurrent and newly diagnosed low-grade gliomas of childhood. J Clin Oncol 11:850-856, 1993
29. Packer RJ, Ater J, Allen J, et al: Carboplatin and vincristine chemotherapy for children with newly diagnosed progressive low-grade gliomas. J Neurosurg 86:747-754, 1997
30. Merchant TE, Kun LE, Wu S, et al: Phase II trial of conformal radiation therapy for pediatric low-grade glioma. J Clin Oncol 27:3598-3604, 2009
31. Lassaletta A, Guerreiro Stucklin A, Ramaswamy V, et al: Profound clinical and radiological response to BRAF inhibition in a 2-month-old diencephalic child with hypothalamic/chiasmatic glioma. Pediatr Blood Cancer 63: 2038-2041, 2016
32. Rush S, Foreman N, Liu A: Brainstem ganglioglioma successfully treated with vemurafenib. J Clin Oncol 31:e159-e160, 2013
33. del Bufalo F, Carai A, Figà-Talamanca L, et al: Response of recurrent BRAFV600E mutated ganglioglioma to vemurafenib as single agent. J Transl Med 12:356, 2014
34. Skrypek M, Foreman N, Guillaume D, et al: Pilomyxoid astrocytoma treated successfully with vemurafenib. Pediatr Blood Cancer 61:2099-2100, 2014
35. Aguilera D, Janss A, Mazewski C, et al: Successful retreatment of a child with a refractory brainstem ganglioglioma with vemurafenib. Pediatr Blood Cancer 63:541-543, 2016

Affiliations

Alvaro Lassaletta, Michal Zapotocky, Matthew Mistry, Vijay Ramaswamy, Marion Honnorat, Rahul Krishnatry, Ana Guerreiro Stucklin, Nataliya Zhukova, Anthony Arnoldo, Scott Ryall, Catriona Ling, Tara McKeown, Jim Loukides, James T. Rutka, Peter Dirks, Michael D. Taylor, Shiyi Chen, Ute Bartels, Annie Huang, Eric Bouffet, Cynthia Hawkins, and **Uri Tabori**, The Hospital for Sick Children, Toronto; **Adam Fleming**, McMaster Children's Hospital, McMaster University, Hamilton; **Shayna Zelcer**, Children's Hospital of

Western Ontario, London, Ontario; **David Eisenstat** and **Bev Wilson**, Stollery Children's Hospital, University of Alberta, Edmonton, Alberta; **Anne Sophie Carret**, Hospital Sainte Justine; **Nada Jabado**, McGill University, Montreal; **Valerie Larouche**, Centre Hospitalier Universitaire de Québec, Québec City, Quebec, Canada; **Ofelia Cruz** and **Carmen de Torres**, Hospital Sant Joan de Déu, Barcelona, Spain; **Cheng-Ying Ho**, University of Maryland School of Medicine, Baltimore, MD; **Roger J. Packer**, Children's National Health System, Washington, DC; **Ruth Tatevossian**, **Ibrahim Qaddoumi**, **Julie H. Harreld**, **James D. Dalton**, and **David W. Ellison**, St Jude Children's Research Hospital, Memphis, TN; **Jean Mulcahy-Levy** and **Nicholas Foreman**, Children's Hospital Colorado, Aurora, CO; **Matthias A. Karajannis**, **Shiyang Wang**, and **Matija Snuderl**, New York University Langone Medical Center, New York, NY; **Amulya Nageswara Rao** and **Caterina Giannini**, The Mayo Clinic, Rochester, MN; **Mark Kieran** and **Keith L. Ligon**, Dana-Farber Cancer Institute, Boston Children's Hospital, Boston, MA; **Maria Luisa Garre**, **Paolo Nozza**, **Samantha Mascelli**, and **Alessandro Raso**, Istituto Giannina Gaslini, Genoa, Italy; **Sabine Mueller** and **Theodore Nicolaides**, University of California, San Francisco, San Francisco, CA; **Karen Silva** and **Romain Perbet**, Hospices Civils de Lyon; **Alexandre Vasiljevic**, **Cécile Faure Conter**, and **Didier Frappaz**, Institute of Pediatric Hematology and Oncology, Lyon, France; **Sarah Leary** and **Courtney Crane**, Seattle Children's Hospital, Seattle, WA; **Aden Chan** and **Ho-Keung Ng**, The Chinese University of Hong Kong, Hong Kong; **Zhi-Feng Shi** and **Ying Mao**, Huashan Hospital, Fudan University, Shanghai, People's Republic of China; **Elizabeth Finch**, University of North Carolina, School of Medicine, Chapel Hill, NC; **Peter Hauser**, Semmelweis University, Budapest, Hungary; and **David Sumerauer** and **Lenka Krskova**, University Hospital Motol, Charles University, 2nd Medical School, Prague, Czech Republic.

Support

Supported by grants from the Government of Canada through Genome Canada and the Ontario Genomics Institute (OGI-121); A Kid's Brain Tumor Cure/PLGA Foundation; the Making Headway Foundation; the Brain Tumour Research Assistance and Information Network; Meagan's Walk Fellowship in Pediatric Neuro-Oncology; Restracomp Scholarship and Fellowship funds from the Garron Family Chair in Childhood Cancer Research at The Hospital for Sick Children (A.L. and M.Z.); a fellowship sponsored by the Society of Neuro-Oncology as an international research development grant (R.K.); National Institutes of Health, National Cancer Institute Grant No. K08-CA193982 (J.M.); the Fondazione Guido Berlucchi (M.L.G.). The French Groupe d'Étude de Neuropathologie Oncologique Pediatrique network is supported by the Institut National du Cancer (Reference No. 2013-113), and the Italian group was supported by the Associazione Italiana per la Ricerca dei Tumori Cerebrali del Bambino.

Prior Presentation

Presented at the 2016 Annual Meeting of the American Society of Clinical Oncology, Chicago, IL, June 3-7, 2016, and the 17th International Symposium on Pediatric Neuro-Oncology. Liverpool, United Kingdom, June 12-16, 2016.

AUTHORS' DISCLOSURES OF POTENTIAL CONFLICTS OF INTEREST

Therapeutic and Prognostic Implications of BRAF V600E in Pediatric Low-Grade Gliomas

The following represents disclosure information provided by authors of this manuscript. All relationships are considered compensated. Relationships are self-held unless noted. I = Immediate Family Member, Inst = My Institution. Relationships may not relate to the subject matter of this manuscript. For more information about ASCO's conflict of interest policy, please refer to www.asco.org/rwc or ascopubs.org/jco/site/ifc.

Alvaro Lassaletta
Consulting or Advisory Role: Mundipharma
Travel, Accommodations, Expenses: Takeda, Shire

Michal Zapotocky
No relationship to disclose

Matthew Mistry
No relationship to disclose

Vijay Ramaswamy
No relationship to disclose

Marion Honnorat
No relationship to disclose

Rahul Krishnatry
No relationship to disclose

Ana Guerreiro Stucklin
No relationship to disclose

Nataliya Zhukova
No relationship to disclose

Anthony Arnoldo
No relationship to disclose

Scott Ryall
No relationship to disclose

Catriona Ling
No relationship to disclose

Tara McKeown
No relationship to disclose

Jim Loukides
No relationship to disclose

Ofelia Cruz
No relationship to disclose

Carmen de Torres
No relationship to disclose

Cheng-Ying Ho
No relationship to disclose

Roger J. Packer
No relationship to disclose

Ruth Tatevossian
No relationship to disclose

Ibrahim Qaddoumi
No relationship to disclose

Julie H. Harreld
No relationship to disclose

James D. Dalton
No relationship to disclose

Jean Mulcahy-Levy
No relationship to disclose

Nicholas Foreman
No relationship to disclose

Matthias A. Karajannis
Research Funding: Novartis, Pfizer

Shiyang Wang
No relationship to disclose

Matija Snuderl
Stock or Other Ownership: Epizyme, Arca Bioharma, Bluebird Bio, Catalyst Pharmaceuticals, Cellceutix, Geron, Ionis Pharmaceuticals, NanoString Technologies, Acceleron Pharma

Amulya Nageswara Rao
No relationship to disclose

Caterina Giannini
No relationship to disclose

Mark Kieran
Consulting or Advisory Role: Novartis, Bayer, Boehringer Ingelheim, Sigma-Tau, Merck
Speakers' Bureau: Merck Sharp & Dohme
Travel, Accommodations, Expenses: Merck Sharp & Dohme

Keith L. Ligon
Stock or Other Ownership: Travera
Research Funding: Plexxikon (Inst), Amgen (Inst), X4 Pharma (Inst), Tragara (Inst)
Patents, Royalties, Other Intellectual Property: Molecular diagnostics assay patent

Maria Luisa Garre
No relationship to disclose

Paolo Nozza
No relationship to disclose

Samantha Mascelli
No relationship to disclose

Alessandro Raso
No relationship to disclose

Sabine Mueller
No relationship to disclose

Theodore Nicolaides
No relationship to disclose

Karen Silva
No relationship to disclose

Romain Perbet
No relationship to disclose

Alexandre Vasiljevic
No relationship to disclose

Cécile Faure Conter
No relationship to disclose

Didier Frappaz
Consulting or Advisory Role: Bristol-Myers Squibb

Sarah Leary
No relationship to disclose

Courtney Crane
No relationship to disclose

Aden Chan
No relationship to disclose

Ho-Keung Ng
No relationship to disclose

Zhi-Feng Shi
No relationship to disclose

Ying Mao
No relationship to disclose

Elizabeth Finch
No relationship to disclose

David Eisenstat
No relationship to disclose

Bev Wilson
No relationship to disclose

Anne Sophie Carret
No relationship to disclose

Peter Hauser
No relationship to disclose

David Sumerauer
No relationship to disclose

Lenka Krskova
No relationship to disclose

Valerie Larouche
No relationship to disclose

Adam Fleming
No relationship to disclose

Shayna Zelcer
No relationship to disclose

Nada Jabado
No relationship to disclose

James T. Rutka
No relationship to disclose

Peter Dirks
No relationship to disclose

Michael D. Taylor
No relationship to disclose

Shiyi Chen
No relationship to disclose

Ute Bartels
No relationship to disclose

Annie Huang
No relationship to disclose

David W. Ellison
No relationship to disclose

Eric Bouffet
Research Funding: Genentech, Bristol-Myers Squibb

Cynthia Hawkins
Research Funding: Bayer
Travel, Accommodations, Expenses: Merck Canada

Uri Tabori
No relationship to disclose

Acknowledgment

Neuropathologic diagnosis for France's cases was performed by the Groupe d'Étude de Neuropathologie Oncologique Pediatrique, and human biological samples and associated data were obtained from Cardiobiotec Biobank (CRB-HCL Hospices Civils de Lyon BB-0033-00046).

Appendix

METHODS

Patient Cohorts

This study was approved by the institutional review board of the Hospital for Sick Children (SickKids). By using our pediatric low-grade glioma (PLGG) database, we retrospectively identified 517 of 845 patients who were diagnosed at SickKids between 1985 and 2015 for whom both biopsy material and adequate clinical follow-up were available. In all patients, BRAF V600E mutation was analyzed. Subependymal giant-cell astrocytomas were excluded from the analysis (517 patients – seven patients with subependymal giant-cell astrocytomas = 510 patients). In those patients who received chemotherapy and had available studies and imaging (computed tomography and/or magnetic resonance imaging) were compared before initiation of treatment and at 6 months of receiving treatment to evaluate the response to chemotherapy for each treatment received. Progression was defined as the need for treatment change related to tumor growth (surgery, chemotherapy, or radiation) after imaging or clinical worsening. To be more accurate in the analysis of global incidence and the incidence according to location and pathology subtypes, we decided to include in this analysis only the total number of patients who were diagnosed from year 2000 (N = 449). We were able to obtain a BRAF mutation status for 90% of patients (n = 405).

Independent Cohort of BRAF V600E-Mutated PLGG

To validate our data of patients with the BRAF V600E-mutation, we retrieved 180 patients with BRAF V600E-mutated PLGG from 18 collaborating centers from around the world. Clinical data collected included the same variables as in our cohort. In all samples received, BRAF V600E mutation was performed for confirmation and CDKN2A copy number status was also assessed by using the same methods as described for our cohort.

Statistical Analysis

To examine the prognostic effect of BRAF V600E, we constructed Cox proportional hazards regression models with and without BRAF V600E, along with other covariates, such as age, gross total resection, CDKN2A, grade, and sex. Concordance probability estimate was calculated as an indicator that assessed the overall value of a covariate in predicting a censored outcome and it was preferred over C-index in the Cox model context. In addition, logistic regression models were performed with and without BRAF V600E. Corresponding C-index values were calculated.

Biologic Studies.

Immunohistochemistry. Detection of BRAF V600E by immunohistochemistry was performed on our Benchmark Ventana Machine (Tucson, AZ) using the Optiview detection kit (Tucson, AZ). CC1 was used for heat retrieval for 40 minutes. Thirty-six minutes of incubation with the Mouse Anti-Human BRAF V600E Monoclonal Antibody from Spring Bioscience (Pleasanton, CA). Casein was used for 8 minutes to help lessen some background staining and hematoxylin counterstain was used for 12 minutes. Slides were scored by a senior neuropathologist at SickKids (C.H.).

Nucleic acid isolation. DNA was first isolated from formalin-fixed, paraffin-embedded (FFPE) tumor tissue using the MasterPure Complete DNA and RNA Purification Kit (MC85200; Epicentre, Madison, WI) according to manufacturer instructions. Total RNA was extracted from FFPE tissue with the RNeasy FFPE extraction kit (Qiagen, Valencia, CA) using manufacturer guidelines.

Droplet digital PCR—rare event detection. In this study, we used droplet digital (dd) PCR (Bio-Rad, Hercules, CA) to detect the somatic point mutation c.1799 C>T in the BRAF gene (p.V600E). The rare event detection assay for BRAF V600E was conducted according to manufacturer instructions. In brief, each 20-μL reaction mixture contained 50 ng DNA, 12.5 μL ddPCR Supermix for probes (no dUTP; Bio-Rad), 1.25 μL PrimePCR ddPCR mutation assay BRAF WT for p.V600E, Human (unique assay ID: dHsaCP2000028), 1.25 μL PrimePCR ddPCR mutation assay BRAF p.V600E, Human (unique assay ID: dHsaCP2000027), and 1 μL Fast Digest BsuRI (Thermo Fisher Scientific Life Sciences, Waltham, MA). PCR reaction mixtures were partitioned into an emulsion of approximately 20,000 uniformly sized droplets. Droplets were then transferred to a 96-well PCR plate, heat sealed, and

placed in a conventional thermal cycler (C1000 Touch Thermal Cycler; Bio-Rad). Thermal cycling conditions were as follows: 95°C for 10 minutes, 39 cycles of 94°C for 30 seconds and 55°C for 60 seconds, 98°C for 10 minutes, and a 4°C hold. After PCR, the PCR plate was loaded on a QX100 droplet reader (QX100 System; Bio-Rad). Analysis of ddPCR data was performed with Quanta-Soft software (Version 1.6.6; Bio-Rad). Each tumor sample was run in technical duplicates.

ddPCR—copy number variation. We also used ddPCR to assess copy number changes in the gene CDKN2A. The assay was performed similarly to the rare event detection assay. We used prime PCR ddPCR copy number assay CDKN2A (unique assay ID: dHsaCP1000581) and a reference prime PCR ddPCR copy number assay APB31 (unique assay ID: dHsaCP2500348). A known homozygous deleted cell line, AM38, was used as a zero-copy control, whereas an Ontario Population Genomics Platform healthy control sample (ID: 85751) obtained from The Center of Applied Genomics at SickKids was used as a two-copy control.

Samples that showed < 1.4 copy number value as calculated from the total target and reference event number were considered deleted (concentration [copies/μL] of target/concentration [copies/μL] of reference $\times$ expected copy number of diploid genome 2). Each sample was run in technical duplicate, which yielded four data points. Final results were determined as the mean copy number of data points that belonged to both the target and reference genes. Thermal cycling conditions were as follows: 95°C for 10 minutes, 39 cycles of 94°C for 30 seconds and 60°C for 60 seconds, 98°C for 10 minutes, and a 4°C hold.

NanoString—detection of fusion transcripts. Probes that targeted KIAA1549-BRAF fusion variants were designed in collaboration with NanoString (Seattle, WA). Five hundred nanograms of total RNA was added to the nCounter Elements TagSet (Seattle, WA) in hybridization buffer and incubated at 67°C for 20 hours. The sample was processed on the nCounter Preparation Station and the cartridge scanned at 555 fields of view on the nCounter Digital Analyzer. Raw counts were subjected to technical normalization by using counts obtained for positive control probe sets included in each run. The statistical outlier detection method was used to detect the presence of an expressed fusion. Data were viewed by using a box plot, and the presence of an extreme outlier ($3\times$ interquartile range) indicates fusion expression.

Fluorescent in situ hybridization. Fluorescent in situ hybridization was designed to detect transcripts by using bacterial artificial chromosome clones within the duplicated region at 7q34 (RP11-248P7 and RP11-837G3) and 7p12.1 control probes (RP11-478M17 and RP11-876P22). Probes were obtained from The Centre for Applied Genomics. The 7q34 clones were directly labeled with Spectrum Green fluorochrome, and control clones were directly labeled with Spectrum Orange fluorochrome. Paraffin fluorescent in situ hybridization analysis was performed on 4-μm tumor sections. Slides were baked overnight to fix the section to the slide and were pretreated by using a paraffin pretreatment kit (Abbott, Chicago IL). Sections were dehydrated before slide/probe codenaturation on thermobrite (Intermedico, Markham, ON, Canada). Denaturation conditions used for paraffin-embedded slides/probes were as follows: 85°C for 7 minutes, followed by overnight incubation at 37°C. Slides were washed in $\times 0.4$ side scatter/0.3% NP-40 at 73°C for 30 seconds, followed by $\times 2$ side scatter/0.1% NP-40 at room temperature for 30 seconds. Slides were counterstained with DAPI. Nuclei were analyzed by using an Axioplan2 epifluorescence microscope (Zeiss, Jena, Germany). Images were captured by an Axiocam MRm Camera (Imaging Associates, Bicester, United Kingdom) and analyzed by using an imaging system with Isis Software (Version 5.1.110; MetaSystems, Boston, MA).

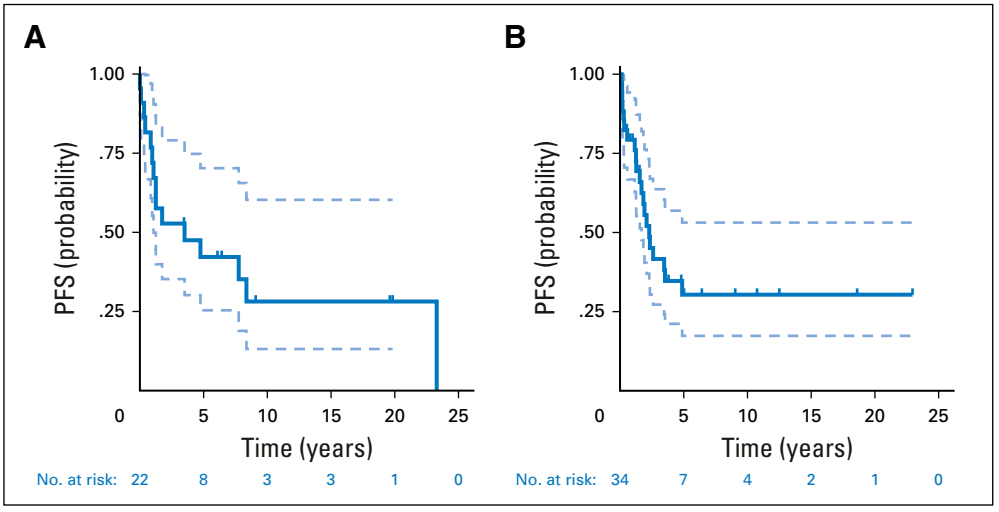

Fig A1. Progression-free survival (PFS) of patients from the SickKids cohort who were treated with conventional therapies. (A) PFS for patients with BRAF V600E from the SickKids cohort who were treated with radiation. (B) PFS for patients with BRAF V600E from the SickKids cohort who were treated with chemotherapy.

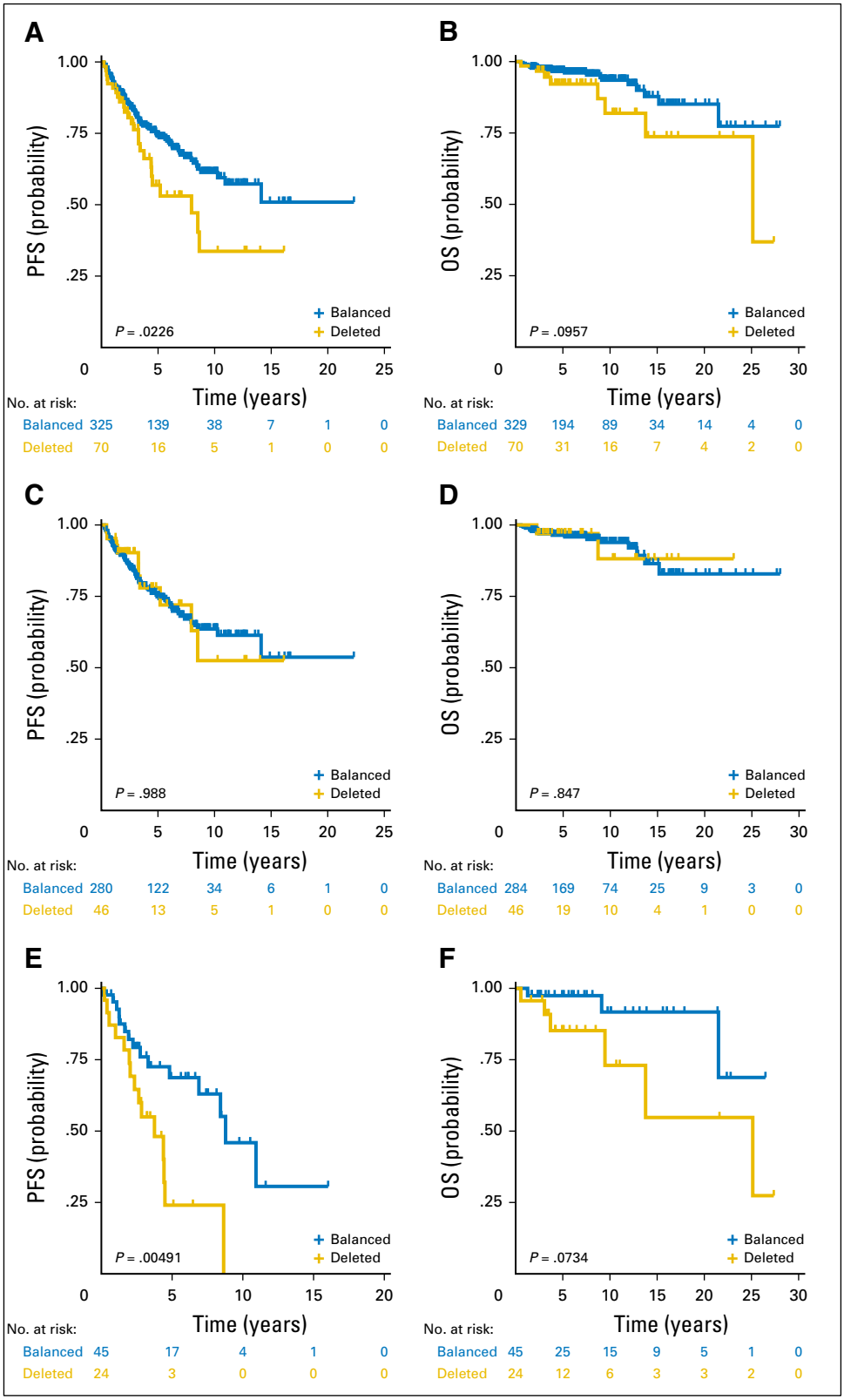

Fig A2. Survival of SickKids patients stratified by *CDKN2A* status. (A) Progression-free survival (PFS) and (B) overall survival (OS) for all patients from the SickKids cohort according to *CDKN2A* status. (C) PFS and (D) OS for patients from the SickKids cohort with wild-type pediatric low-grade glioma (PLGG) according to *CDKN2A* status. (E) PFS and (F) OS for patients from the SickKids cohort with BRAF V600E PLGG according to *CDKN2A* status. *P* values were determined by using log-rank test.

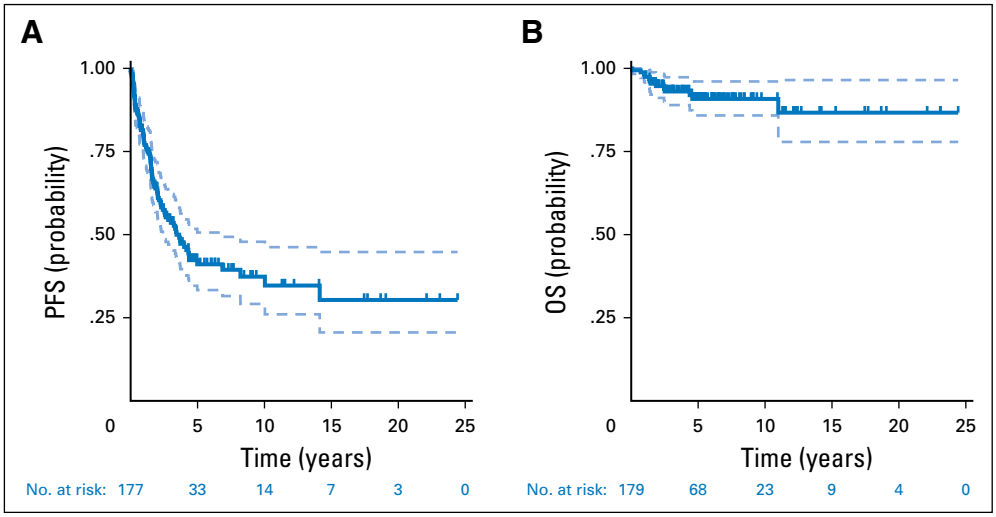

Fig A3. (A) Progression-free survival (PFS) for the BRAF V600E independent cohort. (B) Overall survival (OS) for the BRAF V600E independent cohort.

Table A1. BRAF V600E Mutated Patient Characteristics in the SickKids and Independent Cohorts

Characteristic	SickKids Cohort (n = 99)	Independent Cohort (n = 180)
Sex, %		
Male/female	53/47	48/52
Median age, years (range)	9.23 (0.23-17.46)	9.33
Location, %		
Hemispheres	53.5	52.2
Midline	27.3	23.9
Cerebellar	5.1	11.1
Brainstem	11.1	9.4
Spine	3	0.6
Other		2.8
Diagnosis, %		
Pilocytic astrocytoma	12.1	17.2
Pilomyxoid astrocytoma	2	0.6
Ganglioglioma	33.3	32.8
PXA	10.1	18.9
Diffuse astrocytoma	10.1	6.7
LGG NOS	25.3	13.3
Others	7.1	10.5
OS: Median follow-up, years (range)	5.11 (0.05-27.37)	4.01 (0-24.43)
PFS: Median follow-up, years (range)	2.69 (0.01-16.03)	2.01 (0-24.43)
% of GTR	44.4	42.7
Received treatment other than surgery, %	40.4	42.2
Received radiation, %	22.2	23.8
Transformation, %	4	2.7

Abbreviations: GTR, gross total resection; LGG NOS, low-grade glioma not otherwise specified; OS, overall survival; PFS, progression-free survival; PXA, pleomorphic xanthoastrocytoma.